ELSEVIER

In vivo toxicological effects and spectral studies of new triorganotin(IV)–N-maleoyltranexamates

M.I. Khan [a],*, Musa Kaleem Baloch [a], Muhammad Ashfaq [b], Gerrit Stoter [c]

[a] *Department of Chemistry, Faculty of Sciences, Gomal University, Dera Ismail Khan, N-WFP 75070, Pakistan*
[b] *Department of Chemistry, Islamia University, Bahawalpur, Pakistan*
[c] *Department of Medical Oncology, Daniel den Hoed Cancer Center, Erasmus University Medical Center, Groene Hilledijk 301, 3075 EA Rotterdam, The Netherlands*

Abstract

Multinuclear NMR (^{1}H, ^{13}C and [119]Sn), FT-IR, [119m]Sn Mössbauer spectroscopy, elemental analysis and MS have been carried out for five newly synthesized triorganotin(IV) esters of N-maleoyl-protected tranexamic acid. As per spectroscopic outcome these are five-coordinate polymers with bridging carboxylate group in the solid state, while five-coordinated in trigonal bipyramidal geometry in solution form. Elemental analysis and MS data confirmed the 1:1 ligand to metal ratio and spectroscopic data. These complexes were tested in vitro against various human tumoural cell lines, in vivo in mice and found to be active. Further complexes **4** and **5** showed higher toxicity as compared to complexes **1**–**3** and the ligand. The nature (alkyl/phenyl/aryl) and size of covalently attached R′ groups of Sn(IV) atom and partition coefficients played a key role in the toxicities of the reported complexes.
© 2006 Elsevier B.V. All rights reserved.

Keywords: N-Maleoyltranexamic acid; In vivo anti-tumour; In vitro anti-fungal and anti-leishmanial

1. Introduction

Organotin(IV) compounds being biologically active are extensively used as fungicides, pesticides, anti-fouling coating materials, polymer stabilizers, preservatives for wood, etc. [1–4]. Organotin(IV) esters of carboxylic acids are widely studied due their potential as anti-tumour agents, though, the cause of this activity is still a question to be answered [5–10]. Amino acids and their derivatives are therapeutic molecules and interesting ligands in the coordination chemistry of organotin(IV) carboxylates [11–20]. In order to develop new organotin biocides with bio-active ligands; we have synthesized, characterized and tested the in vitro as well as in vivo anti-tumour activity of five new triorganotin(IV) complexes of therapeutic molecule like tranexamic acid (Fig. 1) [21]. Significant data of the

in vitro screenings prompted us to study the in vivo anti-tumour potential in mice and prospective results ascertained their in vivo implications.

2. Results and discussion

All the reported compounds (**1**–**6**) are non-hygroscopic, quite stable at room temperature, non-crystalline, with good yields (79–93%) and soluble in most organic solvents. The elemental analysis data were in good agreement with the calculated percentages of C, H, N and Sn for all the synthesized complexes.

3. Solid-state spectroscopy

3.1. FT-IR spectroscopic results

The bands associated with N-maleoyl ring are in positions similar to those they occupy as free ligand, thus rules

---

* Corresponding author. Tel.: +92 03219604028; fax: +92 966 750255.
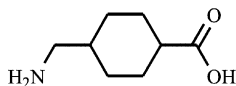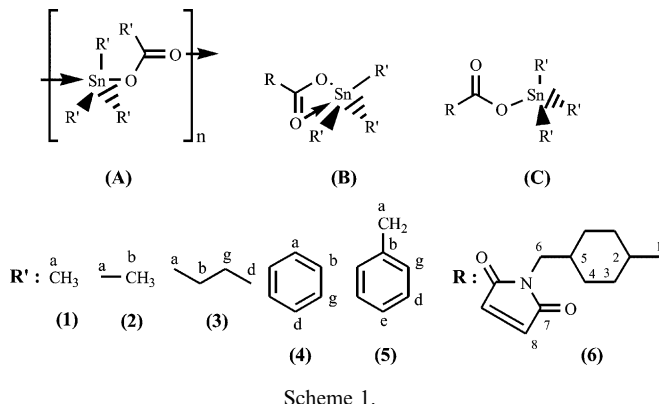 *E-mail address:* chmikhan@hotmail.com (M.I. Khan).

Fig. 1. Molecular structure of tranexamic acid.

Scheme 1.

out any coordination of maleimido C–O to Sn(IV). Characteristic vibrational frequencies have been identified by comparing the spectra of all the complexes with their precursors [9,11–14]. The data are consistent with the formation of well-defined complexes with the composition R'_3SnR, which was confirmed by the presence of Sn–O and Sn–C bonds in the range 516–543 cm^{-1} and 525–542 cm^{-1}, respectively [22–24]. The difference of asymmetric and symmetric vibrational frequencies of carboxylic group, i.e., Δv provide notable information about the molecular arrangement in such complexes; the literature reveals that the complexes where difference of $\Delta v < 350$ cm^{-1} and >200 cm^{-1} exhibit a five-coordinated chain/polymeric structure (structure A in Scheme 1); the ligand's carboxylic group bridges two triorganotin(IV) moieties via oxygen-tin bonds in complexes 2, 3 and 5 [10]. However, when $\Delta v(COO) < 200$ cm^{-1}, the carboxylate group in such complexes can be considered to be practically bidentate indicating chelation; it is suggested that the carboxylic group acts as bidentate in complexes 1 and 4, in a trigonalbipyramidal arrangement (structure B in Scheme 1) [12,25].

3.2. Mössbauer spectroscopy

^{119m}Sn Mössbauer spectroscopy was effectively applied to all the complexes; presenting one penta-coordinated Sn(IV) site. Isomeric shifts (IS) for 1–5 fell in the range 1–1.8 mm s^{-1} lower than that of the parent organotin moieties [24,25]. Isomeric shifts decrease on complexation, as a consequence of rehybridization to higher coordination for Sn(IV) atoms in the complexes, indicating lower s-electron density at the Sn(IV) nucleus in the complexes as compared to the precursor tins [9,12,16]. This can be attributed to the great involvement of d-orbitals, which now take part in the

Sn(IV) hybridization, thus reducing the weight of s-orbitals in the overall hybridization of the metal [21,26,9,27]; similar results have been reported for a great variety of other organotin(IV) compounds [9–14,28]. Quadrupole splitting (QS) values, are not sufficient to characterize a Sn(IV) complex as tetra-, penta- or hexa-coordinated [29]; but a comparison with the reported QS data for analogous compounds [13,14,30], lead to a conclusion that, in the solid state the complexes 1 and 4 are five-coordinated in trigonal bipyramidal geometry (B in Scheme 1) while compounds 2, 3 and 5 are also five-coordinated in chain/polymeric geometry (A in Scheme 1). These results are in full agreement with the structural hypothesis based upon the FT-IR study. We think that such combination of spectroscopic methods in the solid state is important for the detection of coordination modes of hyper-valent organotin(IV) compounds.

4. Solution spectroscopy

4.1. ^1H, ^{13}C and ^{119}Sn NMR spectroscopic results

The published data on solution-state NMR of N-protected amino acids allowed complete assignments of all ^1H and ^{13}C signals in the spectra of *N*-maleoyltranexamic acid [11–14,28]. The integrated intensities in the ^1H NMR spectra clearly indicate a 1:1 metal-to-ligand stoichiometry in solution in agreement with the analytical data on the solids. From the two-bond couplings, $^\alpha J[^{119}Sn-^1H]$, the C–Sn–C angle (θ) was determined using Lockhart's equation (Eq. (1)) [31], the results derived for 1–5 are 107°, 106°, 109°, 111° and 108°, respectively. These results suggested tetrahedral geometry (structure C in Scheme 1) or very weak coordination of carboxylic's oxygen to Sn(IV) (structure B in Scheme 1) for 1–5, in agreement with the conclusions drawn from FT-IR and Mössbauer data.
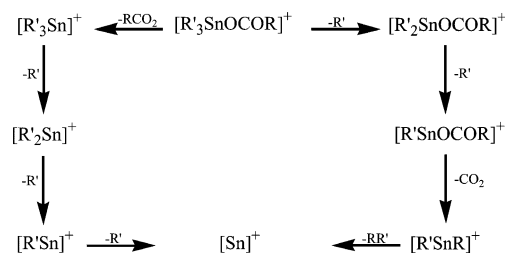
$$\theta = 0.0161[^\alpha J]^2 - 1.32[^\alpha J] + 133.4 \tag{1}$$

In ^{13}C NMR spectroscopy of organotin(IV) complexes, $J[^{119}Sn-^{13}C]$ values of R$'$ provide a simple way for determination of C–Sn–C bond angle in the coordination polyhedra of such complexes [32]. The R$'$ groups attached to Sn(IV) are bonded through sp^2 hybrid orbital of the Sn atom and sp^3 hybrid orbital of the carbon atoms resulting in increase in the $J[^{119}Sn-^{13}C]$ values, thereby indicating a trigonal bipyramidal geometry where R$'$ groups lie in equatorial plane while the ligand in axial position [23,24]. The $J[^{119}Sn-^{13}C]$ provided a trend $^\alpha J > {}^\beta J > {}^\gamma J$, which confirmed trigonal bipyramidal geometry for complexes 4 and 5 (Scheme 1 structure B) [26,9,27]. In ^{13}C NMR the $^\alpha J[^{119}Sn-^{13}C]$ values provide vital information for determining θ(C–Sn–C); substituting $^\alpha J$ values in Eq. (2), θ can be calculated [31]. θ(C–Sn–C) for 1–5 obtained from Eq. (2) were 111°, 132°, 130°, 129° and 136°, respectively, in agreement with the other experimental results, suggesting trigonal bipyramidal geometry (structure B in Scheme 1).

$${}^{\alpha}J = 11.4\theta - 875. \tag{2}$$

Although $\delta({}^{119}\text{Sn})$ is influenced by several factors, including the aromatic or aliphatic nature of R′ group bound to the tin atom (and possibly the type of donor atoms of the ligand), it may be used with caution to infer the coordination number of the tin atom [29,33]. The solution ${}^{119}\text{Sn}$ NMR spectra of all the complexes show just one signal at 134.1, 21.46, 102.35, −118.33 and −88.55 ppm for complexes **1–5**, respectively, which is in accordance with the previous data for analogous penta-coordinated triorganotin(IV) carboxylates indicating weak interactions in trigonal bipyramidal arrangement which may be attributed to solvent effect [6,11–13,27].

In the 70 eV mass spectra of the reported complexes, fortunately molecular ion peaks of medium intensity for **1**, **2** and **5**, while for **3** and **4** weak intensity were seen. Two modes of fragmentation are depicted in Scheme 2 and it was observed that all the complexes obey these modes ably supported by the literature [34]. Primary fragmentation is due to consecutive loss of R′ groups followed by the elimination of CO_2 from the ligand and thereafter remaining part of the ligand leaving Sn^+ as end product. The second proposed route of fragmentation is the loss of CO_2 in the first step, followed by the R′ groups and then the remaining part of the ligand with Sn^+ as a residue (Scheme 2).

5. Bioactivity

All the complexes (**1–5**) and the ligand (**6**) were tested in vitro for their bioavailability, against seven tumoural cell lines of human origin including MCF-7 mammary cancer, EVSA-T mammary cancer, WiDr colon cancer, IGROV ovarian cancer, M19 melanoma, MEL A498 renal cancer and H226 lung cancer. The complexes displayed significant activities in comparison to ligand and the reference drugs (Table 1). Penninks and Seinen [35] suggested that organotin(IV) compounds wield anti-tumour effects through binding to thiol groups of proteins; in contrary, but in analogy with the behavior of several cytotoxic organotin(IV) complexes may interact with DNA [5,28,36]. However, the cause of enhancement in cytotoxicity and exact mechanism of action of such organotin(IV) complexes is still a question to be answered. It has been observed in our complexes that the in vitro toxicity enhances by the bulkiness of R′ groups attached to Sn(IV), against the tumoural cell lines used. To highlight this statement, the average ID_{50} activity data have been plotted versus the percent CH in Fig. 2. The percent CH has been defined as
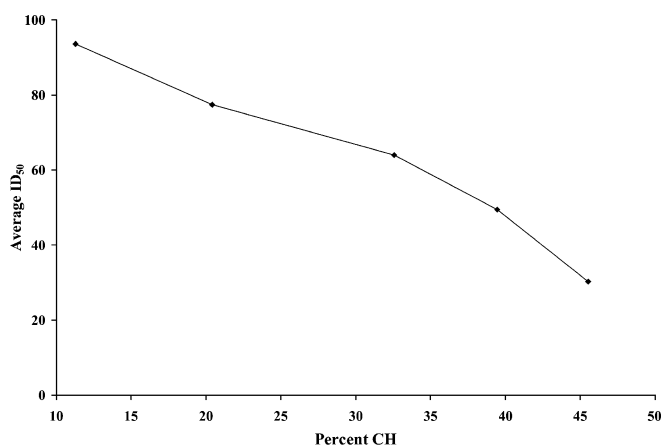

Fig. 2. Average ID_{50} as a function of present CH (Eq. (3)) for the complexes **1–5**.

Scheme 2.

Table 1
In vitro inhibition doses (ng/ml) of compounds **1–6** against seven tumoural cell lines of human origin

	A498	EVSAT	H226	IGROV	M19	MCF7	WiDr
1	93	82	66	112	105	96	101
2	86	80	77	101	100	30	68
3	77	81	30	83	101	24	52
4	70	42	21	80	93	17	23
5	50	33	5	12	89	6	17
6	333	241	239	655	348	200	302
Dox	28	44	68	107	23	35	62
Cpt	1432	658	471	478	321	214	105
5-FU	2214	325	164	205	301	54	82
MTX	3094	210	65	25	212	100	64
ETO	514	531	438	328	155	84	103

MCF-7 (mammary cancer), EVSA-T (mammary cancer), WiDr (colon cancer), IGROV (ovarian cancer), M19 (melanoma), MEL A498 (renal cancer) and H226 (lung cancer), Do (doxorubicin), Cp (cisplatin), 5-Fu (5-fluorouracil), Mt (methotrexate) and Et (Etopside).

$$\text{Percent CH(R}') = \frac{(C_n \times 12.011) + (H_n \times 1.0079)}{\text{Molecular mass of the complex}} \times 100,$$

$$(3)$$

where n is the number of carbon or hydrogen atoms in R′ groups. Fig. 2 shows that ID_{50} decreases with the increase in percent CH almost linearly. However, some deviations in case of alkyl R′ groups have been observed, which may be attributed to variation in conformational behavior and distribution of complexes between different phases. Since it is difficult to judge the bioactivity of any compound by a single factor, hence we have tried another important parameter, partition coefficient; the ID_{50} values have been plotted versus it (see Fig. 3). It is interesting to note that the data of complexes **1**–**5** prove that ID_{50} values decrease linearly with the increase in partition coefficient. This is certainly encouraging for us that the major controlling parameter seems to be P_{ow} (partition coefficient in octanol/water system) or in other words the polarizability of R′–Sn bond induced by R′ groups. It can be therefore concluded that in complexes **1**–**5**, hydrophillicity increases with the bulkiness of R′ groups, which enhances the partition coefficient, thereby boosting up the bioactivity. We can say that the increase in hydrophillicity of these complexes might be responsible for such significant results as observed by others [14–19]. It is stated for information that Sn–C polarity (Bz > Ph > Bu > Et > Me) is in the same order. Conclusively, we can say that the bulkiness of the attached R′ group/percent CH values are interlinked with each other, which enhances the polarity and partition function of the complexes. The increase in partition function provides the complexes an opportunity to interact with the target thereby resulting enhancement in activity.

5.1. Anti-tumour activity on mice

Initial dose-finding studies were performed with groups of 2 mice, which were treated for two weeks by i.p. Injections (qd7×2). Results are shown in Figs. 4–9 for compounds **1**–**6**.
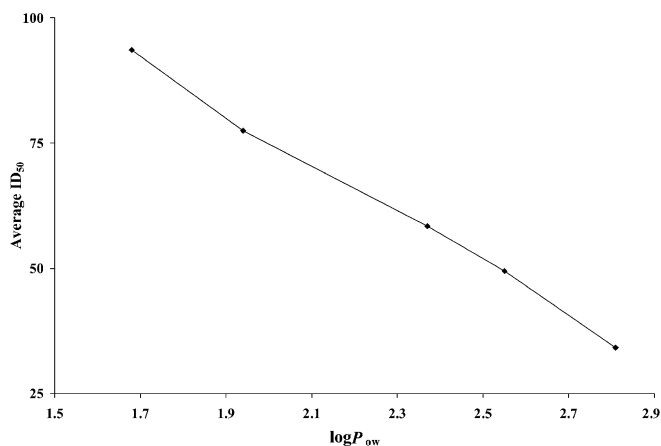

Fig. 3. Dependence of average ID_{50} over Partition coefficients of complexes **1**–**5**.
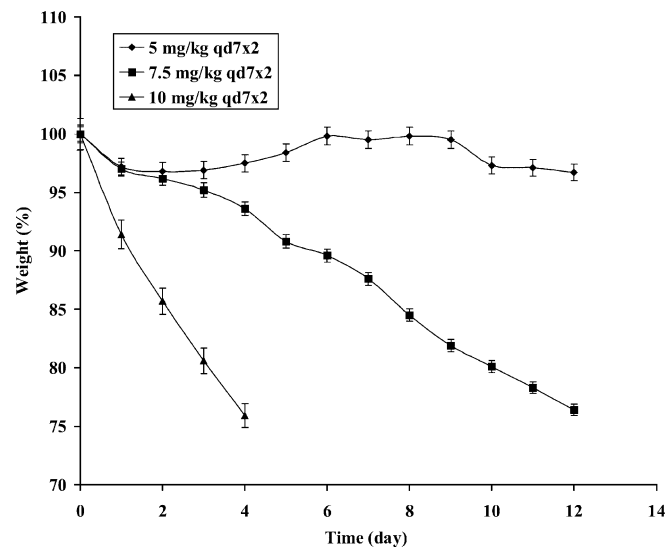

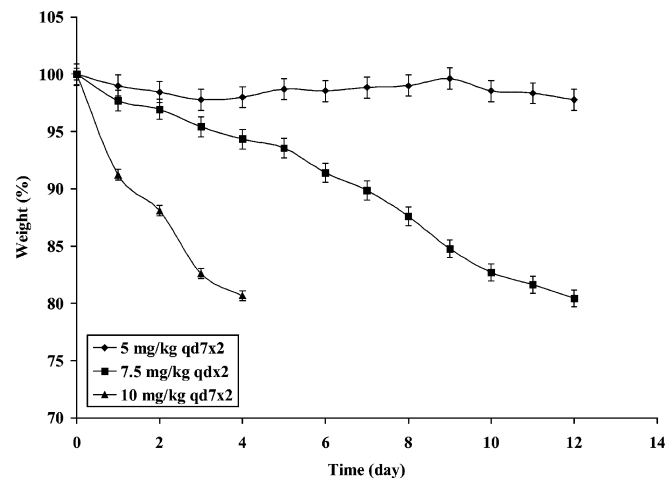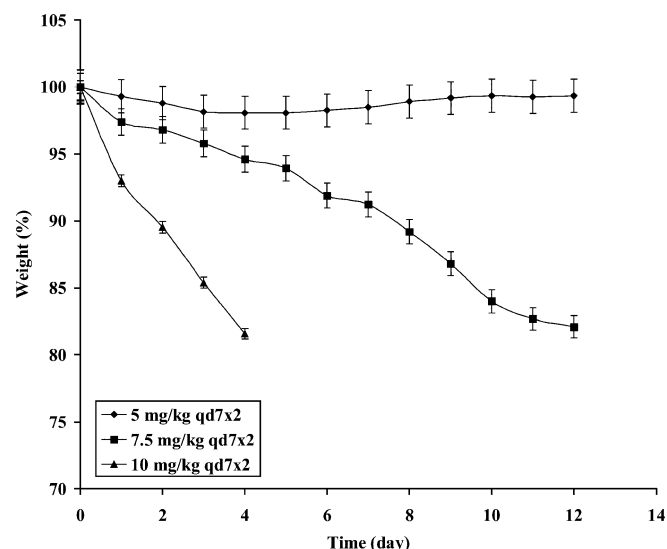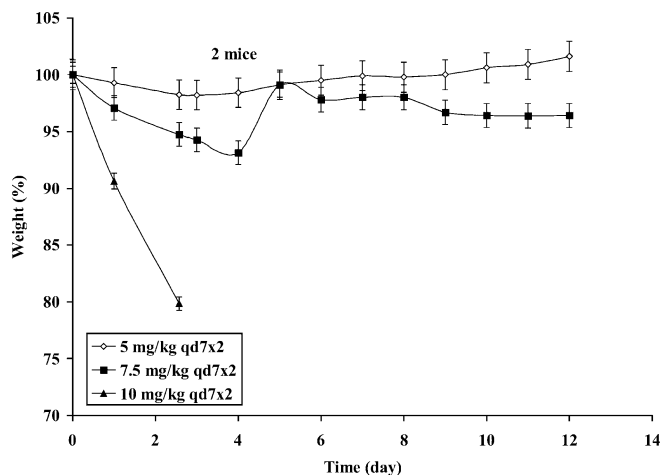Fig. 4. Dose-finding study for **1**.

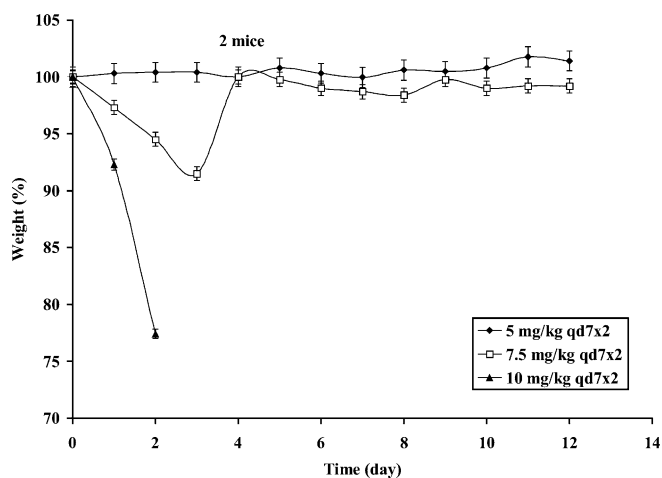
Fig. 5. Dose-finding study for **2**.

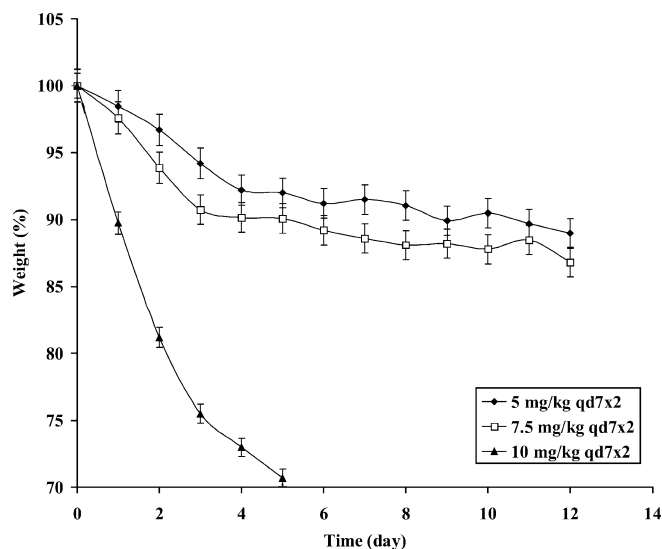Fig. 6. Dose-finding study for **3**.

Fig. 7. Dose-finding study for **4**.

Based on results obtained in dose-finding studies, for each compound, a dose was chosen somewhat lower than the MTD dose, since experience with previous compounds demonstrated more toxicity in tumour bearing mice [11,12]. However, the toxicity in tumour (colon 26A) bearing Balb/C mice was unexpectedly high as shown in Figs. 10–12. For compounds **4** and **5**, severe toxicities were observed just after one injection. Therefore, administration of a second injection of these compounds was not acceptable. However, for compounds **1**, **2**, **3**, and **6** mice could be treated twice. To further elaborate the dose impact, the initial slopes of the plots (Figs. 4–9) have been calculated and scaled with the dose of the given compound. The results so obtained are plotted in Fig. 13 and extrapolated to zero dose value. Thus, we can conclude that the impact goes down with the increase in dose value and most of the drugs work well up
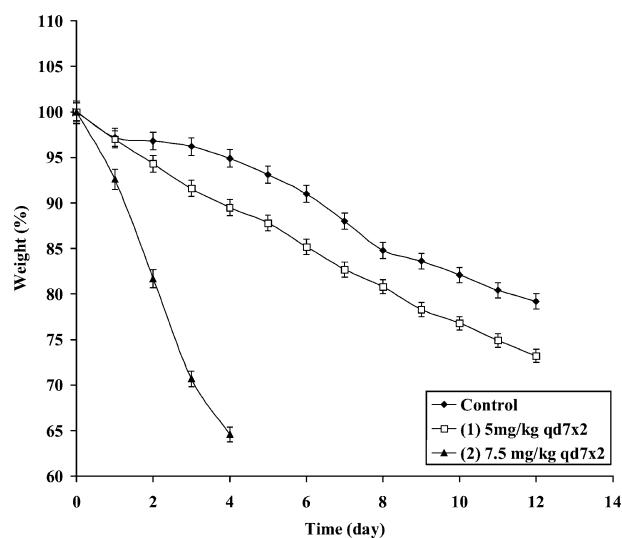

Fig. 8. Dose-finding study for **5**.

Fig. 10. Weight loss for Balb/C (colon 26A) induced by **1** and **2**.

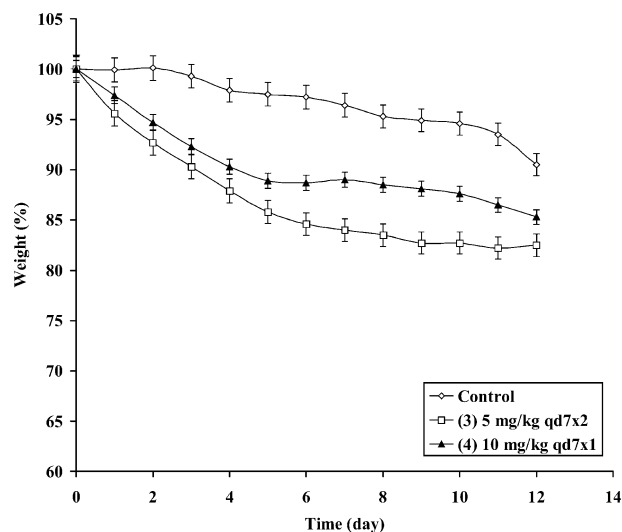Fig. 9. Dose-finding study for **6**.

Fig. 11. Weight loss for Balb/C (colon 26A) induced by **3** and **4**.
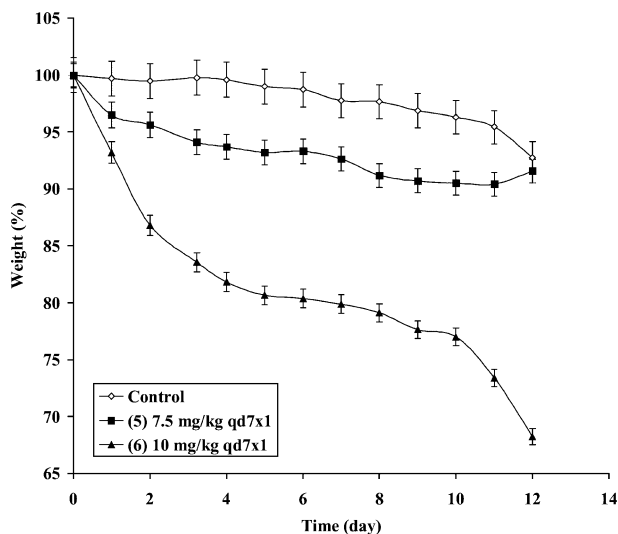
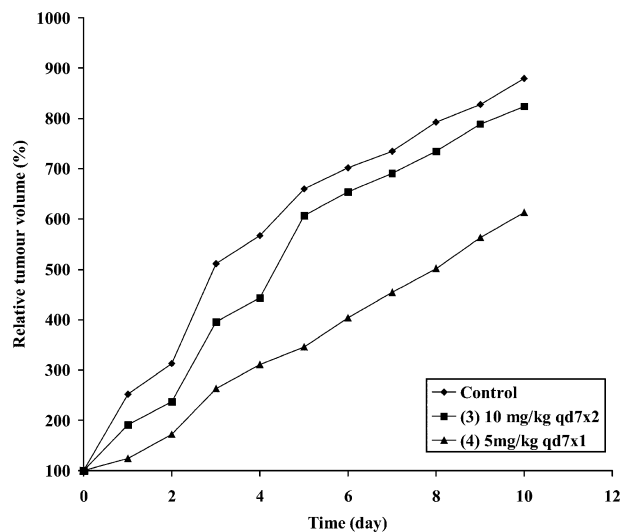Fig. 12. Weight loss for Balb/C (colon 26A) induced by **5** and **6**.
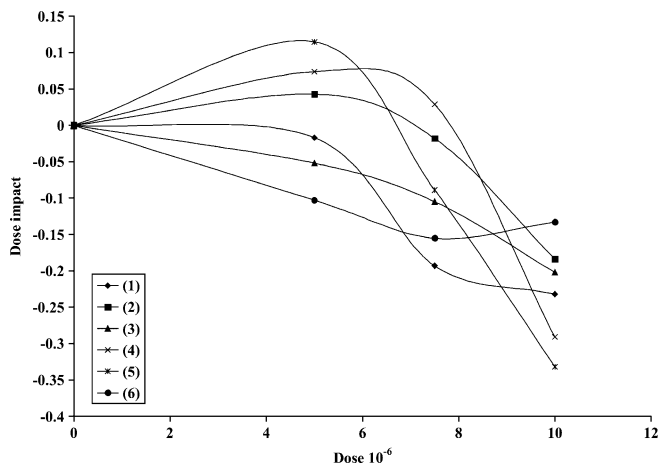

Fig. 13. Dose impact of **1**–**6**.

Fig. 14. Anti-tumour activity of **1** and **2** against colon 26A in Balb/C mice.
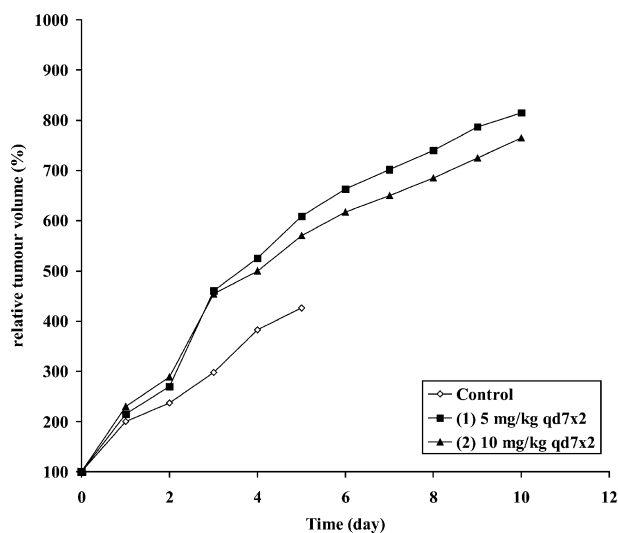

Fig. 15. Anti-tumour activity of **3** and **4** against colon 26A in Balb/C mice.
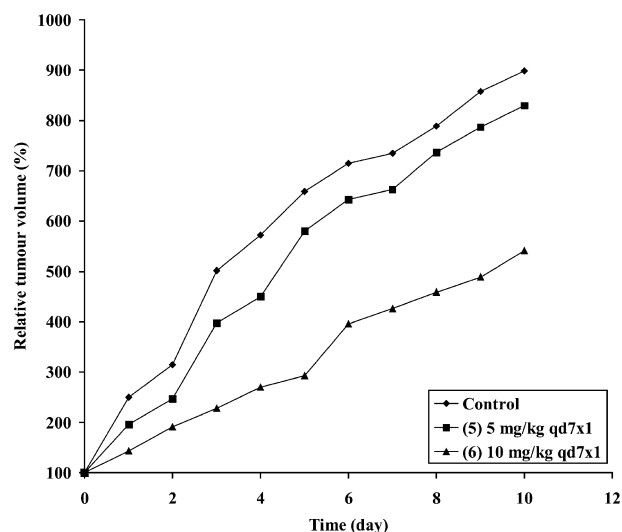
Fig. 16. Anti-tumour activity of **5** and **6** against colon 26A in Balb/C mice.

to 7.5 mg/kg. However, for the increase in dose leads to either death of the mice or its positive impact is not up to the expected mark. For example, in case of compounds **1**, **2**, **3** and **6** the dose impact is quite low in case of 10 mg/kg as compared to 5 or 7.5 mg/kg.

5.2. In vivo anti-tumour activity on mice

Although the compounds were too toxic to administer according to the scheduled use in the dose-finding study, conclusions have been drawn on a single dose treatment of the colon 26A bearing mice. The assumption was made that even at this high dose no anti-tumour activity is present; it would be unlikely to that lower doses at a schedule of qd7×2 would be able to produce anti-tumour effect.

At their MTD no anti-tumour effects were seen for **1, 2, 3, 6**, i.e., the T/C ≈ ⩾ 1 (Figs. 10,11 and 14,15,16). The compounds **4** and **5** displayed clear activity after single dose administration (for **4** and **5** T/C equals 0.67 and 0.32, respectively).

It is to be noted that the in vitro studies also show a similar trend confirming the dependence of toxicity over the attached R′ groups.
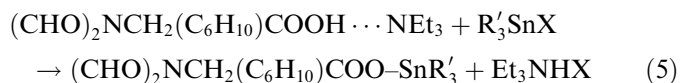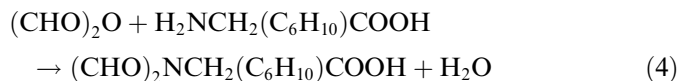
6. Conclusions

Spectroscopically authenticated organotin(IV) complexes of *N*-maleoyl-protected tranexamic acid are described for the first time in this paper. Characterization of these coordinated complexes shows that Sn(IV) atom is penta-coordinated in trigonal bipyramidal/polymeric arrangement in solid and solution. Most of these in general and triphenyl- and tribenzylSn(IV) complexes in particular displayed promisingly significant in vitro and in vivo anti-tumour activities and are of practical interest for in vivo testing on human tumoural cell lines.

7. Experimental

7.1. Material and methods

Maleic anhydride, trimethyltin(IV)chloride, tri-*n*-butyltin(IV)chloride, triphenyltin(IV)chloride, tricyclohexyltin(IV)chloride, and triethylamine were procured from commercial sources (AR Grade, Aldrich Chemicals) used as such, while tribenzyltin(IV)chloride was prepared as reported [37]. Tranexamic acid was a gift from Tabros Pharma. Pakistan. Solvents used during this work were dried according to reported methods [38]. The ligand was synthesized as described elsewhere (Eq. (4)) [39]; while the complexes were synthesized as given in Eq. (5) [12]. Partition coefficient measurements were made in octanol/water system according reported procedure [38].

$$(CHO)_2O + H_2NCH_2(C_6H_{10})COOH$$
$$\rightarrow (CHO)_2NCH_2(C_6H_{10})COOH + H_2O \quad (4)$$

$$(CHO)_2NCH_2(C_6H_{10})COOH \cdots NEt_3 + R'_3SnX$$
$$\rightarrow (CHO)_2NCH_2(C_6H_{10})COO-SnR'_3 + Et_3NHX \quad (5)$$

7.2. Instrumentation

Elemental analyses (C, H, N) were performed on a Yanaco high-speed CHN analyzer; antipyrene was used as a reference, while tin content was estimated according to reported procedures [40]. Uncorrected melting points were taken on a Reichert Thermovar of F.G. Bode Co., Austria.

The FT-IR spectra of the ligand and the complexes were measured on a Bruker FT-IR spectrophotometer TENSOR27 using OPUS software in the range of 5000–500 cm^{-1}.

^{1}H, and ^{13}C NMR spectra in deuterated chloroform (CDCl$_3$) were recorded on a multinuclear Bruker *Biospin* AMX 300 MHz FT NMR spectrometer operating at room temperature (300 MHz for ^{1}H and 75 MHz for ^{13}C); the proton and carbon chemical shifts were measured with respect to SiMe$_4$. ^{119}Sn NMR spectra in CDCl$_3$ were recorded at 186.50 MHz on a Bruker AMX 500 spectrophotometer using 5 mm o.d. tubes and are reported relative to external neat SnMe$_4$ (δ^{119}Sn = 0 ppm).

For Mössbauer measurements, the solid samples were maintained at liquid nitrogen temperature (77.3 K), V.G. Micromass 7070 F Cryolid liquid nitrogen cryostat. The multichannel calibration was performed with an enriched iron foil using ^{57}Co–Pd source, while the zero point of the Doppler velocity scale was determined through the absorption spectra of CaSnO$_3$ (^{119}Sn = 0.5 mg cm^{-2}). The resulting 5×105 – count spectra were refined to obtain the isomeric shift, IS (mm s^{-1}), the nuclear quadrupole splitting QS, ρ (mm s^{-1}) and the width at half-height of the resonant peaks, Γ (mm s^{-1}).

Mass spectra were recorded using model MAT 112 and 113, Double-Focusing Mass Spectrometer (Finnigan) connected to IBM at compatible PC based system.

7.3. In vitro anti-tumour activity on human tumoural cell lines

The compounds **1**–**6** were screened in vitro against seven human cancer cell lines, i.e., MCF-7 mammary cancer, EVSA-T mammary cancer, WiDr colon cancer, IGROV ovarian cancer, M19 melanoma, MEL A498 renal cancer and H226 lung cancer, reference drugs used are doxorubicin (Do), cisplatin (Cp), 5-fluorouracil (5-Fu), methotrexate (Mt). The screening was performed with aqueous solutions containing 1% DMSO or ethanol by the literature procedure [41]. In vitro inhibition doses (ID$_{50}$ ng/ml) are presented in Table 1.

7.4. In vivo anti-tumour activity

The experimental conditions for in vivo cytotoxicity are already described elsewhere [12,41,42]. Briefly, the test compounds were dissolved in DMSO to a concentration ranging from 50 to 100 mg/ml and diluted to 10 mg/ml in arachidis oil, which was also used for further dilutions. DMSO acidified or alkalined to get a clear solution. The amount of DMSO could not be increased since mice did not tolerate more than 1%. Mice were injected intra-peritoneally. The MTD was defined as the dose resulting in 10–15% weight loss, while T/C is the ratio of the tumour size of the Treated mice to that of the control mice expressed in %.

8. Spectroscopic data

For numbering (NMR) and MS fragments see Schemes 1 and 2, respectively.

8.1. [(CH₃)₃SnOCOR] (1)

8.1. [(CH$_3$)$_3$SnOCOR] (1)

Recrystallization: C_6H_6/C_6H_{12}, yield: 79%, mp 87 °C. Found: C, 45.00, H, 3.76, N, 3.48; Sn, 29.65%. $C_{15}H_{23}NO_4Sn$ requires: C, 45.03; H, 3.79; N, 3.50; Sn, 29.67.

v_{max}/cm^{-1} 533 (Sn–O), 537 (Sn–C), 1545$_s$, 1718$_{asym}$ (C=O), 173 (Δv).

^{119m}Sn Mössbauer/mm s^{-1}: QS: 3.61, IS: 1.19; Γ_1: 0.71, Γ_2: 0.69, ρ = QS/IS: 3.03.

δ_H 2.32 (H2, m), 2.26 (H3, m), 1.69 (H4, m), 1.78 (H5, m), 3.31 (H6, t), 6.88 (H8, s), 0.04 (Hα, s, $^\alpha J(^{119}Sn–^1H) = 37.3$).

δ_C 184.35 (C1), 45.86 (C2), 24.76 (C3), 28.47 (C4), 32.51 (C5), 41.80 (C6), 173.05 (C7), 136.68 (C8), 0.21 (Cα, $^\alpha J(^{119}Sn–^{13}C) = 387$).

δ ^{119}Sn 134.1.

m/z [EI]: 400 (23%, M$^{+\cdot}$), 385 (43%, M$^+$–R′), (M$^+$–2R′), 370 (20%, M$^+$–3R′), 355 (38%, M$^+$–R), 119 (Sn$^+$, 9%).

8.2. [(Et₃)₃SnOCOR] (2)

8.2. [(Et$_3$)$_3$SnOCOR] (2)

Recrystallization: C_6H_6/C_6H_{12}, yield: 83%, mp 125–127 °C. Found: C, 48.88, H, 6.59, N, 3.15, Sn, 26.81%. $C_{18}H_{29}NO_4Sn$ requires: C, 48.90, H, 6.61, N, 3.17, Sn, 26.85.

v_{max}/cm^{-1} 531 (Sn–O); 544 (Sn–C); 1529$_s$, 1732$_{asym}$(C=O); 203 (Δv).

^{119m}Sn Mössbauer/mm s^{-1}: QS: 3.42, IS: 1.36, Γ_1: 0.87, Γ_2: 0.59; ρ = QS/IS: 2.51.

δ_H 2.32 (H2, m), 2.26 (H3, m), 1.69 (H4, m), 1.78 (H5, m), 3.31 (H6, t), 6.88 (H8, s), 0.88 (Hα, q, $^\alpha J(^{119}Sn–^1H) = 41.53$), 0.71 (Hβ, t).

δ_C 187.22 (C1), 46.42 (C2), 25.37 (C3), 30.46 (C4), 33.55 (C5), 42.03 (C6), 174.16 (C7), 135.63 (C8), 2.65 (Cα, $^\alpha J(^{119}Sn–^{13}C) = 634$), 9.04 (Cβ, $^\beta J(^{119}Sn–^{13}C) = 362$).

δ ^{119}Sn 21.46.

m/z [EI]: 442 (23%, M$^{+\cdot}$), 413 (31%, M$^+$–R′), 384 (8%, M$^+$–2R′), 355 (20%, M$^+$–3R′), 206 (64%, M$^+$–R), 119 (11%, Sn$^+$).

8.3. [(Bu₃)₃SnOCOR] (3)

8.3. [(Bu$_3$)$_3$SnOCOR] (3)

Recrystallization: $C_6H_{12}/CHCl_3$, yield: 87%, mp 93 °C. Found: C, 54.75, H, 7.83, N, 2.63, Sn, 22.52%. $C_{24}H_{41}NO_4Sn$ requires: C, 54.77, H, 7.85, N, 2.66, Sn, 22.56.

v_{max}/cm^{-1} 522 (Sn–O), 536 (Sn–C), 1520$_s$, 1756$_{asym}$(C=O); 236 (Δv).

^{119m}Sn Mössbauer/mm s^{-1}: QS: 3.15, IS: 1.52, Γ_1: 0.98, Γ_2: 0.84, ρ = QS/IS: 2.07.

δ_H 2.34 (H2, m), 2.31 (H3, m), 1.54 (H4, m), 1.69 (H5, m), 3.27 (H6, t), 6.92 (H8, s), 0.86 (Hα, m, $^\alpha J(^{119}Sn–^1H) = 27.85$), 0.71 (Hβ, q), 1.36 (Hγ, m), 0.98 (Hδ, t).

δ_C 188.07 (C1), 46.23 (C2), 25.52 (C3), 31.22 (C4), 33.48 (C5), 42.37 (C6), 174.31 (C7), 135.46 (C8), 15.42 (Cα, $^\alpha J(^{119}Sn–^{13}C) = 602$), 21.31 (Cβ, $^\beta J(^{119}Sn–^{13}C) = 334$), 27.04 (Cγ, $^\gamma J(^{119}Sn–^{13}C) = 241$), 14.68 (Cδ, $^\delta J(^{119}Sn–^{13}C) = 55$).

δ ^{119}Sn 102.35.

m/z [EI]: 526 (4%, M$^{+\cdot}$), 469 (9%, M$^+$–R′), 412 (13%, M$^+$–2R′), 355 (47%, M$^+$–3R′), 290 (13%, M$^+$–R), 119 (53%, Sn$^+$).

8.4. [(Ph₃)₃SnOCOR] (4)

8.4. [(Ph$_3$)$_3$SnOCOR] (4)

Recrystallization: $CHCl_3/C_6H_6$, yield: 80%, mp 181 °C. Found: C, 61.43, H, 4.97, N, 2.37, Sn, 20.24%. $C_{30}H_{29}NO_4Sn$ requires: C, 61.46, H, 5.21, N, 2.39, Sn, 20.25.

v_{max}/cm^{-1} 512 (Sn–O), 531 (Sn–C), 1567$_s$, 1761$_{asym}$ (C=O), 194 (Δv).

^{119m}Sn Mössbauer/mm s^{-1}: QS: 3.22; IS: 1.43; Γ_1: 0.84; Γ_2: 0.76; ρ = QS/IS: 2.25.

δ_H 2.29 (H2, m), 2.37 (H3, m), 1.43 (H4, m), 1.61 (H5, m), 3.33 (H6, t), 6.83 (H8, s), 7.71 (Hβ, m, $^\beta J$ ^{119}Sn–^{1}H = 29.48), 7.43 (Hγ, m), 7.55 (Hδ, m).

δ_C 183.93 (C1), 46.47 (C2), 25.66 (C3), 30.64 (C4), 32.87 (C5), 42.75 (C6), 176.08 (C7), 134.22 (C8), 135.63 (Cα, $^\alpha J(^{119}Sn–^{13}C) = 598$), 138.07 (Cβ, $^\beta J(^{119}Sn–^{13}C) = 580$), 131.04 (Cγ, $^\gamma J(^{119}Sn–^{13}C) = 221$), 128.41 (Cδ, $^\delta J(^{119}Sn–^{13}C) = 55$).

δ ^{119}Sn −118.33.

m/z [EI]: 586 (7%, M$^{+\cdot}$), 509 (10%, M$^+$–R′), 432 (69%, M$^+$–2R′), 355 (43%, M$^+$–3R′), 351 (66%, M$^+$–R), 119 (37%, Sn$^+$).

8.5. [(Benz₃)₃SnOCOR] (5)

8.5. [(Benz$_3$)$_3$SnOCOR] (5)

Recrystallization: $CHCl_3/C_6H_6/CH_2Cl_2$, yield: 84%, mp 161 °C. Found: C, 63.06, H, 5.59, N, 2.20, Sn, 18.85%. $C_{33}H_{35}NO_4Sn$ requires: C, 63.08, H, 5.61, N, 2.23, Sn, 18.89.

v_{max}/cm^{-1} 520 (Sn–O), 544 (Sn–C), 1553$_s$, 1741$_{asym}$(C=O), 181 (Δv).

^{119m}Sn Mössbauer/mm s^{-1}: QS: 3.04, IS: 1.59, Γ_1: 0.76, Γ_2: 0.64, ρ = QS/IS: 1.91.

δ_H 2.34 (H2, m), 2.15 (H3, m), 1.67 (H4, m), 1.80 (H5, m), 3.29 (H6, t), 7.62 (H8, s), 2.77 (Hα, m, $^\alpha J$ ^{119}Sn–^{1}H = 31.27), 7.30 (Hγ, m), 7.23 (Hδ, m), 7.27 (Hε, m).

δ_C 188.04 (C1), 47.20 (C2), 25.32 (C3), 31.43 (C4), 34.12 (C5), 42.75 (C6), 172.33 (C7), 130.11 (C8), 17.81 (Cα, $^\alpha J(^{119}Sn–^{13}C) = 672$), 141.02 (Cβ, $^\beta J(^{119}Sn–^{13}C) = 611$), 127.45 (Cγ, $^\gamma J(^{119}Sn–^{13}C) = 221$), 128.66 (Cδ, $^\delta J(^{119}Sn–^{13}C) = 55$), 121.58 (Cε).

δ ^{119}Sn −88.55.

m/z [EI]: 628 (51%, M$^{+\cdot}$), 537 (48%, M$^+$–R′), 446 (07%, M$^+$–2R′), 355 (47%, M$^+$–3R′), 392 (33%, M$^+$–R), 119 (29%, Sn$^+$).

8.6. [(CHCO)₂NCH₂C₆H₁₀COOH] (6)

Recrystallization: C_6H_6, yield: 93%, mp 89–91 °C. Found: C, 60.73, H, 6.35, N, 5.87%. $C_{12}H_{15}NO_4$ requires: C, 60.75, H, 6.37, N, 5.90.

v_{max}/cm^{-1} 3100–3450 (COOH), 1673$_s$, 1736$_{asym}$(C=O), 63 (Δv).

δ_H 2.43 (H2, m), 2.20 (H3, m), 1.72 (H4, m), 1.84 (H5, m), 3.33 (H6, t), 6.97 (H8, s).

δ_C 185.12 (C1), 45.79 (C2), 25.27 (C3), 28.43 (C4), 32.56 (C5), 41.87 (C6), 171.84 (C7), 135.29 (C8).

Acknowledgements

References

[1] K.C. Molloy, in: F.R. Hartley (Ed.), The Chemistry of Metal–Carbon Bond, vol. 5, Wiley, New York, 1996.

[2] N.F. Cardarelli, in: Tin as Vital Nutrient, first ed., CRC Press, Boca Raton, FL, 1986.

[3] E.R.T. Tiekink, in: Trends in Organometallic Chemistry, vol. 1, Council of Scientific Research Integration, Trivandrum, India, 1994.

[4] P.D. Lickiss, in: P.J. Smith (Ed.), Chemistry of Tin, second ed., Balckie, London, 1998.

[5] M. Gielen, J. Bra. Chem. Soc. 14 (6) (2003) 870.

[6] M. Gielen, P. Lelieveld, D. de Vos, R. Willem, in: B.K. Keppler (Ed.), Metal Complexes in Cancer Chemotherapy, VCH, Weinheim, 1993.

[7] M. Boualam, M. Gielen, A. Meriem, D. de Vos, R. Willem, B.V. Phamachemie, Eur. Publ. 472 783, Appl. 90/202, 316.7 (1992).

[8] M. Gielen, Appl. Organomet. Chem. 16 (2002) 481.

[9] L. Pellerito, L. Nagy, Coord. Chem. Rev. 224 (2002) 111.

[10] M. Gielen, M. Biesemans, D. de Vos, Appl. Organomet. Chem. 19 (2005) 440.

[11] M.I. Khan, M.K. Baloch, M. Ashfaq, J. Organomet. Chem. 689 (2004) 3370.

[12] M.I. Khan, M.K. Baloch, M. Ashfaq, G.J. Peters, Appl. Organomet. Chem. 19 (2005) 132.

[13] M. Ashfaq, M.I. Khan, M.K. Baloch, A. Malik, J. Organomet. Chem. (2004) 238.

[14] M. Ashfaq, A. Majeed, A. Rauf, A.W.K. Khanzada, W.U. Shah, M.I. Ansari, Bull. Chem. Soc. Jpn. 72 (9) (1999) 2073.

[15] M. Pervez, S. Anwar, A. Badshah, B. Ahmad, A. Majeed, M. Ashfaq, Acta Crystallogr., Sect. C 56 (2000) 59.

[16] A. Pellerito, T. Fiore, A.M. Giuliani, F. Maggio, L. Pellerito, R. Vitturi, M.S. Colomba, R. Barbieri, Appl. Organomet. Chem. 11 (1997) 601.

[17] Y. Zhou, T. Jiang, S. Ren, J. Yu, Z. Xia, J. Organomet. Chem. 690 (2005) 2186.

[18] J.S. Casas, A. Castiñeiras, F. Condori, M.D. Couce, U. Russo, A. Sánchez, R. Seoane, J. Sordo, J.M. Varela, Polyhedron 22 (2003) 53.

[19] D. Zuo, T. Jiang, H. Guan, K. Wang, X. Qi, Z. Shi, Molecules 6 (2001) 647.

[20] H.D. Yin, Q.B. Wang, S.C. Xue, J. Organomet. Chem. 690 (2005) 435.

[21] British Pharmacopoeia, vol. 1, 6th Ed., Stationary Office, UK, 1999.

[22] A. Szorcsik, L. Nagy, L. Pellerito, T. Yamaguchi, K. Yoshida, J. Radioanal. Nucl. Chem. 256 (2003) 3.

[23] G.K. Sandhu, S.P. Verma, Polyhedron 2830 (1987) 587.

[24] M.J. Hynes, M. O'Dowd, J. Chem. Soc., Dalton Trans. 563 (1987).

[25] T.S.B. Baul, W. Rynjah, E. Rivarola, A. Linden, J. Organomet. Chem. 690 (2005) 613.

[26] E.R.T. Tiekink, Trend Organomet. Chem. 1 (1994) 71.

[27] M. Gielen, A.E. Khloufi, M. Biesemans, F. Keyser, R. Willem, Appl. Organomet. Chem. 7 (1993) 201.

[28] A. Jancso, L. Nagy, E. Molderheim, E. Sletten, J. Chem. Soc., Dalton Trans. 1587 (1999).

[29] J. Holecek, K. Handlir, M. Nadvornik, A. Lycka, J. Organomet. Chem. 315 (1986) 299.

[30] R. Barbieri, L. Pellirito, G. Ruisi, M. LoGiudice, F. Huber, G. Atassi, Inorg. Chim. Acta 66 (1982) L39.

[31] T.P. Lockhart, W.F. Manders, Inorg. Chem. 25 (1986) 892.

[32] M. Kemmer, L. Ghys, M. Gielen, M. Biesemans, E.R.T. Tiekink, R. Willem, J. Organomet. Chem. 582 (1999) 195.

[33] E.R. Tiekink, J. Organomet. Chem. 408 (1991) 323.

[34] R.H. Petrucci, General Chemistry: Principals and Modern Application, Macmillan, New York, 1994.

[35] A.H. Penninks, W. Seinen, Vet. Q. 6 (1984) 209.

[36] B.K. Keppler, in: Metal Complexes in Cancer Therapy, VCH, Weinheim, 1993.

[37] K. Sisido, Y. Takeda, Z. Kinngawa, J. Am. Chem. Soc. 83 (1961) 538.

[38] B. Furniss, A.J. Hannaford, P.W.G. Smith, A.R. TatchellVogel's Text Book of Practical Organic Chemistry, vol. 5, ELBS Longman Group, UK, 1989.

[39] O. Keller, J. Rudinger, Helv. Chim. Acta 58 (1975) 531.

[40] J. Mendham, R.C. Denney, J.D. Barnes, M. Thomas, in: Vogel's Text Book of Quantitative Chemical Analysis, sixth ed., Pearson Education Pvt. Ltd., Singapore, 2003.

[41] V.T. De Vita Jr., S. Hellman, S.A. Rosenberg, in: Cancer: Principles and Practice of Oncology, fifth ed., Lippincott/Raven, Philadelphia, PA/New York, 1997.

[42] M. Gielen, R. Willem, A. Bouhdid, D. de Vos, C. Kuiper, M. Veerman, G.J. Peters, Oncol. Rep. 59 (1996) 327.